Atmos. Chem. Phys. Discuss., 10, 21683–21696, 2010
www.atmos-chem-phys-discuss.net/10/21683/2010/
doi:10.5194/acpd-10-21683-2010

Atmospheric
Chemistry
and Physics
Discussions

Effects of ship wakes on ocean brightness and radiative forcing over ocean

C. K. Gatebe[1,2], R. Poudyal[2,3], E. Wilcox[2,*], and J. Wang[2,4]

[1]Goddard Earth Sciences and Technology Center, University of Maryland, Baltimore County, Baltimore, Maryland 21228, USA
[2]NASA Goddard Space Flight Center, Greenbelt, Maryland 20771, USA
[3]Science Systems and Applications, Inc., Lanham, Maryland 20706, USA
[4]University of Nebraska-Lincoln, 303 Bessey Hall Lincoln, Nebraska, 68588-0340, USA
[*]present address: Desert Research Institute, Reno, Nevada 89512, USA

Received: 2 August 2010 – Accepted: 2 September 2010 – Published: 17 September 2010

Correspondence to: C. K. Gatebe (charles.k.gatebe@nasa.gov)

Published by Copernicus Publications on behalf of the European Geosciences Union.

Abstract

Changes in surface albedo represent one of the main forcing agents that can counteract, to some extent, the positive forcing from increasing greenhouse gas concentrations. Here, we quantify the changes in ocean surface albedo from ship wakes and provide an estimate of radiative forcing over the global oceans. Our analysis is based on airborne radiation measurements over the Pacific Ocean near the California coast, where we determined that a ship wake increases reflected sunlight by more than 100% in some cases. Based on registered ships of 100 000 gross tonnage (GT), and assuming a global distribution of 30 000 ships, we estimated the global radiative forcing of ship wakes to be $-0.003\,\mathrm{W\,m^{-2}}$, which is comparable to the forcing of aircraft contrails, but not anticipated in the Intergovernmental Panel on Climate Change (IPCC) 2007 assessment report. From these results, we conclude that the climate impacts associated with ships will become more significant with growing ship traffic.

1 Introduction

The oceanic surface albedo plays a key role in determining the energy exchange between atmosphere and ocean and is, therefore, important for the coupling of atmosphere and ocean models (Li et al., 2006). The albedo regulates the Earth's climate and an increase in surface albedo can counteract, to some extent, the warming due to the positive forcing of increasing greenhouse gases (Menon et al., 2010). The albedo change over land caused by land use and land cover modifications is well documented (Forster et al., 2007). However, modification of the ocean albedo by human activities is unknown, even though the oceans cover 70% of the Earth's surface. This study provides new insights into ship-generated disturbances on the ocean surface, which have received little attention in climate studies, but is potentially significant for the ocean-atmosphere energy balance and could affect climate.

A moving ship generates a wake that is characterised by surface waves, white-water, propeller-generated vortices and submerged bubbles (Reed and Milgram, 2002). Ship wakes can often be seen in images acquired by microwave synthetic aperture radar (SAR) aboard aircraft and satellites (Garzelli, 1995; Munk et al. 1987). The region around and behind the ship, up to a distance of several ship lengths (local wave disturbance region), shows a complex combination of breaking bow and stern waves, depending on the speed, the shape and the propulsion system of the ship (Lyden et al., 1988). Studies have shown that the optical variations observed within ship wakes are largely due to the generation of copious amounts of air bubbles in the upper ocean, a fraction of which accumulate as foam at the surface, where they release scavenged surfactants (Zhang et al., 2004, 1998; Stramski, 1994). The optical effects of surface waves, submerged bubbles and vortices trailing the ship can be observed 5–15 km behind the ship (Munk et al., 1987).

2 Observational assessment of ship wake impacts on surface albedo

During the Arctic Research of the Composition of the Troposphere from Aircraft and Satellites (ARCTAS; 24 June 2008) experiment (Jacob et al., 2010), while flying in the NASA P-3B aircraft (Fig. 1a) over the Pacific Ocean off the coast of southern California, we discovered, serendipitously, enhanced surface reflectance exceeding 100% above normal in most cases in wakes trailing large commercial vessels. The flight was designed primarily for characterising the emissions from cargo ships plying the area, which are known to contribute to air quality problems in California (Corbett and Fishbeck, 2000; Corbett et al., 2007), and the ocean bidirectional reflectance distribution function (BRDF). The aircraft was equipped with instruments to measure gases, aerosols and radiation. As part of the instrument suite, the NASA's Cloud Absorption Radiometer (CAR; Fig. 1b) (Gatebe et al., 2005, 2003; King et al., 1986), which detected the enhanced reflectance, was mounted in the nose cone measuring both transmitted and reflected radiances while scanning perpendicular to the flight direction at a rate of 100 scans a minute. CAR scans through 190° from straight above, through the horizon to straight down. Data were recorded for 14 narrow spectral bands located in the ultraviolet, visible and near-infrared regions in the electromagnetic spectrum (0.340–2.301 µm). Given that the instrument has an instantaneous field-of-view of 1°, a wide scan range of 190°, and assuming an altitude of 300 m above the surface, the diameter of the footprint straight below the aircraft is ∼5 m, increasing to ∼174 m at a viewing zenith angle of 80° from nadir. Therefore, a complete circular orbit by the aircraft allows the CAR to image the surface and sky in all viewing zenith and azimuthal angles, and covering an area defined by a diameter of 4–5 km on the surface (Fig. 1c). We believe that using the CAR in this manner is the most mobile and efficient way of measuring full surface BRDF (Gatebe et al., 2005). Several orbits over the ocean were completed both before and after the arrival of a ship to the sampling area helping to detect change in surface albedo due to ship wakes.

The signature of the ship and its wake can be seen clearly when comparing the BRDF of the case without and with ship wake. We use measurements of BRDF to determine the enhanced reflectance attributable to the presence of ship wake. Figure 2 shows ocean reflectance at 0.870 µm in all viewing azimuth directions (depicted as angle around the polar plot with the solar principal plane at 0°) and viewing zenith angle (depicted as distance from the center of the polar plot) from nadir up to 10° below the horizon. At 0.870 µm, which is widely used in remote sensing over the ocean under clear-sky, effects of atmospheric absorption and scattering can be assumed to be minimal. The unique feature of these BRDF measurements is that reflected solar radiation was observed at a fine angular resolution (1°). As expected, the radiation field over the ocean is characterised by the presence of sunglint with maximum reflectance coinciding with the solar direction (in this case ∼35° elevation angle) viewed towards the sun and minimum reflectance occurring at the same elevation angle viewed away from the sun caused by the aircraft shadow. However, the contrast between Fig. 2a (case without ship wake) and Fig. 2b (case with the ship wake) reveals: (a) ship and ship wakes clearly enhance surface reflectance, (b) the glint is confined over a narrower angular range from the solar principal plane in the ship wake case, and extends farther out towards the horizon, and (c) the glint in the ship wake case has higher reflectance magnitude than the non-ship wake case, which is not so obvious in the figure because of the color scheme used. The narrowing of the angular extent of the glint and the reduction in reflectance in some viewing angles is more than compensated by enhanced surface reflectance at other viewing angles.

The ship passage (Fig. 3a) was captured by the CAR instrument during a ∼2 min interval as seen in the quick-look RGB image shown in Fig. 3b ($R = 1.04\,\mu$m, $G = 0.87\,\mu$m, and $B = 0.47\,\mu$m). The sun can be seen in the sky, well above the horizon, and the sunglint pattern appears very bright against a dark ocean surface. The ship and its wake appear in the quick-look image more clearly at 22:27:58 UTC. The ship appears as a bright dot off the solar principal plane and the ship wake is superimposed on the glint following the ship. Figure 3c (blue curve) shows the mean percentage differences in spectral surface reflectance viewed in the direction of the sunglint between the case with ship wake (22:27:58 UTC–22:29:56 UTC) and the case without the wake (22:23:37 UTC–22:25:44 UTC), normalized to the case without the wake. The green line in Fig. 3c, is similar to the blue line but for a different ship wake viewed in non-glint directions >90° away from the solar principal plane. We identified other ship wakes associated with trailing ships of varying size and observed by CAR at different distances behind the ships; the results are summarized in Table 1. (Note that results for ship wake 4 and 5 are shown in Fig. 3c (green and blue curves, respectively.) Except for the UV reflectances measured for ships 4 and 5, enhanced reflectances were measured across the spectrum from UV to near-IR for all observed wakes, with considerable variability between different wakes.

From the BRDF measurements, we derived spectral albedo (Gatebe et al., 2005) for the ship wake case 5 (with and without wake) by integrating the reflection function over solid angles and subtracting the two cases, then dividing the difference by the albedo of the case without ship wake (cf. Fig. 3c, red dotted curve and Table 1). The corresponding relative enhancements in spectral albedo, representing an ocean area

>13 km^2 as defined by the diameter of the circular aircraft flight path (>4 km), range between 1% and 4% in the visible and near-infrared wavelengths, which is significant given that the integration of the measured BRDF includes large areas not affected directly by the ship wake. The relative enhancement in the ultraviolet (UV) is very small and within the noise owing to low UV reflectance.

3 Estimate and significance of direct radiative forcing of ship wakes

We now explore the impact on climate associated with the strong increase of albedo by ship wakes as a primer for any future work on this serendipitous discovery. To estimate the ship wake impact on climate, we first conclude (based upon the above analysis and the following) that wakes of each ship at any given time increase the ocean albedo (ΔA) by 3% over a 13 km^2 area. This is based on a nominal broadband ocean albedo of about 7% (Zhang et al., 2004) and a conservatively selected 37% relative enhancement of ocean reflectance by ship wakes, which is the minimum change in reflectance observed at 0.340 µm (Table 1; ship wake). Further, the area of modified ocean surface can be deduced by assuming that a ship wake can last for 3–45 min (Zhang et al., 2004; US Patent 5787048 – Ship wake signature suppression: http://www.patentstorm.us/patents/5787048/description.html), and hence, a typical cargo ship of 100 m wide with a speed of 10 m/s can result in a ship wake area of 1.4 km^2 (assuming an average lifetime of 24 min); this estimated ship wake (only) area is consistent with that (ship-wake only area) deduced from CAR observations, and hence, implies that a 3% for ΔA over a 13 km^2 (ship wake and vicinity) area is representative for a ship wake over the open ocean. The number of ships is based on Eyring et al. (2005) who reported 89,843 ships exceeding 100 gross tonnage (excluding submarines) in 2001 operating between 4000 and 6000 h per year depending on size. Allowing that 40% of that operating time may be maneuvering or stationary in port (Endresen et al., 2003) yields approximately 30 000 ships operating in open water. Note that the size of the fleet has quadrupled in approximately 50 years (Buhaug et al., 2009).

Based on the above, and an assumption that the presence of ships is uncorrelated with cloud cover, the direct radiative forcing of the ship wakes in global and annual average would be: 1367 $\mathrm{Wm^{-2}}$ (solar constant) ×0.25 (factor for normalizing the solar constant to the Earth surface) ×0.4 (cloud-free fraction) ×0.03 (albedo increase) ×30 000 (number of ships) ×13 $\mathrm{km^2}$ (area affected by a wake)/(5.1×10^8 $\mathrm{km^2}$ – Earth surface area) ≈0.0031 $\mathrm{Wm^{-2}}$, assuming that the ships are homogeneously distributed over the globe. Since the majority of ships are in the Northern Hemisphere mid-latitude oceans, the lower bound of this estimate averaged over the globe would be 0.0031 $\mathrm{Wm^{-2}}$ ×0.5 (hemispheric factor) $\times\cos\pi/4$ (mid-latitude factor)=0.0011 $\mathrm{Wm^{-2}}$. Consequently, the forcing averaged only over the Northern Hemisphere ocean would be ∼0.0037 $\mathrm{Wm^{-2}}$ (noting that ocean surface area in Northern Hemisphere is ∼30% of the total Earth's surface area). Therefore, either globally or hemispherically, the above estimate of ship wake forcing falls in the IPCC reported range (0.0003–0.03 $\mathrm{Wm^{-2}}$) for the aircraft contrails, and hence, could lead to climate change (Forster et al., 2007), but of a different nature than that from CO_2. Regionally, in harbours and coastal regions, we would expect this forcing to be one order of magnitude larger, that is, 0.037 $\mathrm{Wm^{-2}}$, which is about 2% of more homogeneously-distributed anthropogenic radiative forcing of CO_2 (1.66 $\mathrm{Wm^{-2}}$) measured against the pre-industrial atmosphere. These estimates are designed to be illustrative of the potential magnitude of forcing by ship wakes.

4 Conclusions

While wherever possible we have taken the nominal values for all parameters in our radiative forcing estimate for ship wakes, we admit that some parameters may have large and yet difficult-to-quantify uncertainties. Further sampling of ship wakes is warranted to better constrain the estimated change in albedo from wakes and to improve our understanding of the persistence of the albedo perturbation after passage of the ship. Hence, the forcing estimated here should be considered as a first order estimate (or back-of-the-envelope calculation), whereby uncertainties could be as large as those in the forcing estimate for contrails. But, considering that the global shipping fleet has rapidly grown in the last 5 decades and this trend is likely to continue because of the need of more inter-continental transportation as a result of economic globalization, we argue that the radiative forcing of wakes is expected to be increasingly important to offset to some extent the forcing of greenhouse gases, and hence, should be considered as equally important as the forcing of contrails in the climate modelling and IPCC assessments. These results will have bearing on the suggested geo-engineering schemes (such as using cloud modifying ships) for reducing warming (MacCraken, 2009; E. Kintisch, Could Tiny Bubbles Cool the Planet, SCIENCENOW: http://news.sciencemag.org/sciencenow/2010/03/could-tiny-bubbles-cool-the-plan.html).

Acknowledgements. This research was supported by the Science Mission Directorate of the National Aeronautics and Space Administration as part of the Radiation Sciences Program under Hal B. Maring and Airborne Science Program. This work was performed under NASA Grant NNX08AF89G.

References

Buhaug, Ø., Corbett, J. J.; Endresen, Ø., et al.: Second IMO GHG study, Prevention of air pollution from ships, International Maritime Organization (IMO) London, UK, 2009.

Corbett, J. J. and Fischbeck, P. S.: Emissions from waterborne commerce in United States continental and inland waters, Environ. Sci. Technol., 34, 3254–3260, 2000.

Corbett, J. J. and Kohler, H. W.: Updated emissions from ocean shipping, J. Geophys. Res., 108, doi:10.1029/2003JD003751, 2003.

Corbett, J. J., Firestone, J. and Wang, C.: California Air Resources Board Report, available at: http://www.arb.ca.gov/research/seca/jcfinal.pdf, 2007.

Endresen, Ø, Sørgård, E., Sundet, J. K., Dalsøren, S. B., Isaksen, I. S. A., Berglen, T. F., Gravir, G.: Emission from international sea transportation and environmental impact, J. Geophys. Res., 108, 4560, doi:10.1029/2002JD002898, 2003.

Eyring, V., Köhler, H. W., van Aardenne, J., and Lauer, A.: Emissions from international shipping: 1. The last 50 years, J. Geophys. Res., 110, D17305, doi:10.1029/2004JD005619, 2005.

Forster, P., Ramaswamy, V., Artaxo, P., et al.: Changes in Atmospheric Constituents and in Radiative Forcing, in: Climate Change 2007: The Physical Science Basis. Contribution of Working Group I to the Fourth Assessment Report of the Intergovernmental Panel on Climate Change, edited by: Solomon, S., Qin, D., Manning, M., Chen, Z., Marquis, M., Averyt, K. B., Tignor, M., and Miller, H. L., Cambridge University Press, Cambridge, United Kingdom and New York, NY, USA, 2007.

Garzelli, A.: Detection of ship wakes in SAR images using morphological operators, Comput. Geosci. 21, 1201–1203, 1995.

Gatebe, C. K., King, M. D., Lyapustin, A. I., Arnold, G. T., and Redemann, J.: Airborne Spectral Measurements of Ocean Directional Reflectance, J. Atmos. Sci., 62, 1072–1092, 2005.

Gatebe, C. K., King, M. D., Platnick, S., Arnold, G. T., Vermote, E. F., and Schmid, B.: Airborne spectral measurements of surface-atmosphere anisotropy for sev-eral surfaces and ecosystems over southern Africa, J. Geophys. Res., 108, 8489, doi:10.1029/2002JD002397, 2003.

Jacob, D. J., Crawford, J. H., Maring, H., Clarke, A. D., Dibb, J. E., Emmons, L. K., Ferrare, R. A., Hostetler, C. A., Russell, P. B., Singh, H. B., Thompson, A. M., Shaw, G. E., McCauley, E., Pederson, J. R., and Fisher, J. A.: The Arctic Research of the Composition of the Troposphere from Aircraft and Satellites (ARCTAS) mission: design, execution, and first results, Atmos. Chem. Phys., 10, 5191–5212, doi:10.5194/acp-10-5191-2010, 2010.

King, M. D., Strange, M. G., Leone, P., and Blaine, L. R.: Multiwavelength Scanning Radiometer for Airborne Measurements of Scattered Radiation within Clouds, J. Atmos. Ocean. Technol. 3, 513–522, 1986.

Scinocca, J., Lazare, M., Mcfarlane, N., von Salzen, K., and Solheim, L.: Ocean surface albedo and its impact on radiation balance in climate models, J. Climate, 19, 6314–6333, 2006.

Lyden, J. D., Hammond, R. R., Lyzenga, D. R., and Shuchman, R. A., (1988), Synthetic aperture radar imaging of surface ship wakes, J. Geophys. Res., 93, 12293–12303, 1988.

MacCraken, M. C.: On the possible use of geoengineering to moderate specific climate change impacts, Environ. Res. Lett., 4, 045107, available at: stacks.iop.org/ERL/4/045107, 2009.

Menon, S., Akbari, H., Mahanama, S., Sednev, I., and Levinson, R.: Radiative forcing and temperature response to changes in urban albedos and associated CO_2 offsets, Environ. Res. Lett., 5, 014005, doi:10.1088/1748-9326/5/1/014005, 2010.

Munk, W. H., Scully-Power, P., and Zachariasen, F.: Ships from space, Proceedings of the Royal Society of London. Series A, Mathematical and Physical Sciences, 412(1843), 231–254, 1987.

Reed, A. M. and Milgram, J. H.: Ship wakes and their radar images, Annu. Rev. Fluid Mech., 34, 469–502, 2002.

Stramski, D.: Gas microbubbles, an assessment of their significance to light scattering in quiescent seas, In, Ocean Optics XII, J. S. Jaffe, ed., Proc. SPIE, 2258, 704–710, 1994.

Zhang, X., Lewis, M., Bissett, W. P., Johnson, B., and Kohler, D.: Optical influence of ship wakes, Appl. Optics, 43, 3122–3132, 2004.

Zhang, X., Lewis, M. R., and Johnson, B. D.: Influence of bubbles on scattering of light in the ocean, Appl. Optics, 37, 6525–6536, 1998.

Table 1. Relative Increase in Ocean Reflectance due to Ship Wake.

Relative Change (%): $((Rw - R)/R)^* \cdot 100$										
λ (µm)	0.340	0.381	0.472	0.682	0.870	1.036	1.219	1.273	2.102	Alt (m)/ SZA(°)
ship-1	353	612	796	1157	1101	1031	901	960	600	1324/21
ship-2	109	180	326	552	538	550	522	533	348	1691/20
ship-3	143	297	389	622	683	600	569	749	547	2979/20
ship-4	37	53	192	315	313	283	271	271	240	7093/19
ship-5	78	86	106	126	130	130	126	127	131	297/34
albedo (ship5)	−0.44	−0.10	0.95	1.18	1.73	2.44	2.87	1.79	3.73	

[*] Rw = ship wake reflectance, R = ocean reflectance; SZA = solar zenith angle.

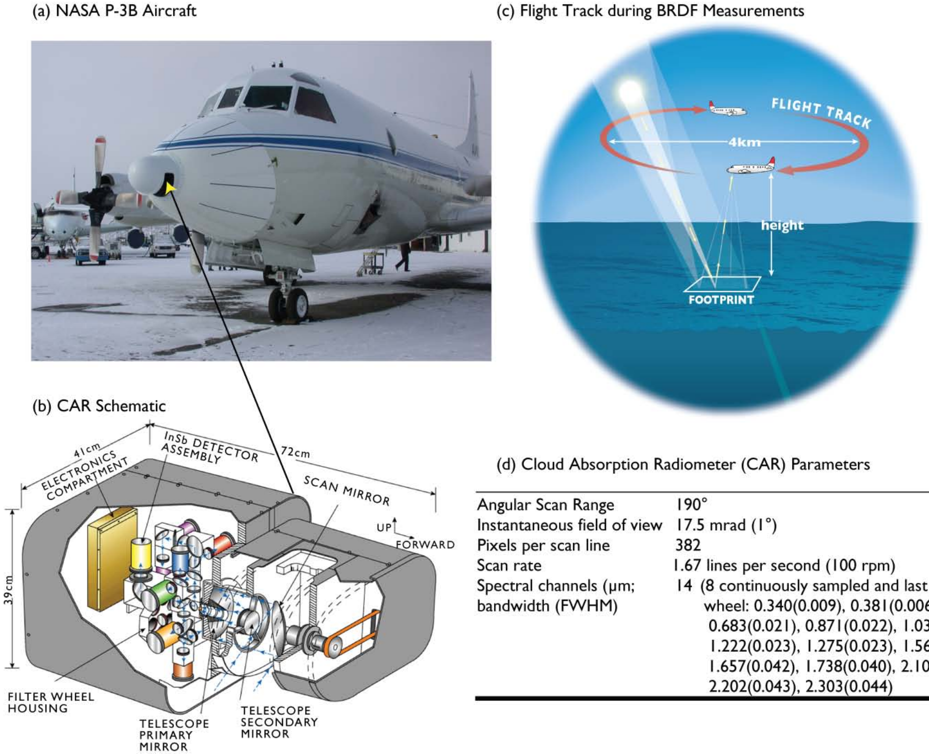

(d) Cloud Absorption Radiometer (CAR) Parameters

Angular Scan Range	190°
Instantaneous field of view	17.5 mrad (1°)
Pixels per scan line	382
Scan rate	1.67 lines per second (100 rpm)
Spectral channels (µm; bandwidth (FWHM)	14 (8 continuously sampled and last six in filter wheel: 0.340(0.009), 0.381(0.006), 0.473(0.021) 0.683(0.021), 0.871(0.022), 1.037(0.021), 1.222(0.023), 1.275(0.023), 1.564(0.032), 1.657(0.042), 1.738(0.040), 2.105(0.045), 2.202(0.043), 2.303(0.044)

Fig. 1. **(a)** The NASA P-3B at NASA Ames, California, USA in June 2008 during ARCTAS Field Experiment. **(b)** Schematic of NASA's Cloud Absorption Radiometer (CAR), which is mounted in the nose cone of the NASA P-3B aircraft. **(c)** Illustration of a clockwise circular flight track that was used for measuring surface bidirectional reflectance distribution function (BRDF) over the Pacific **(d)**. The CAR has 14 narrow spectral bands between 0.34 and 2.30 µm, and flew two missions over the Pacific during ARCTAS.

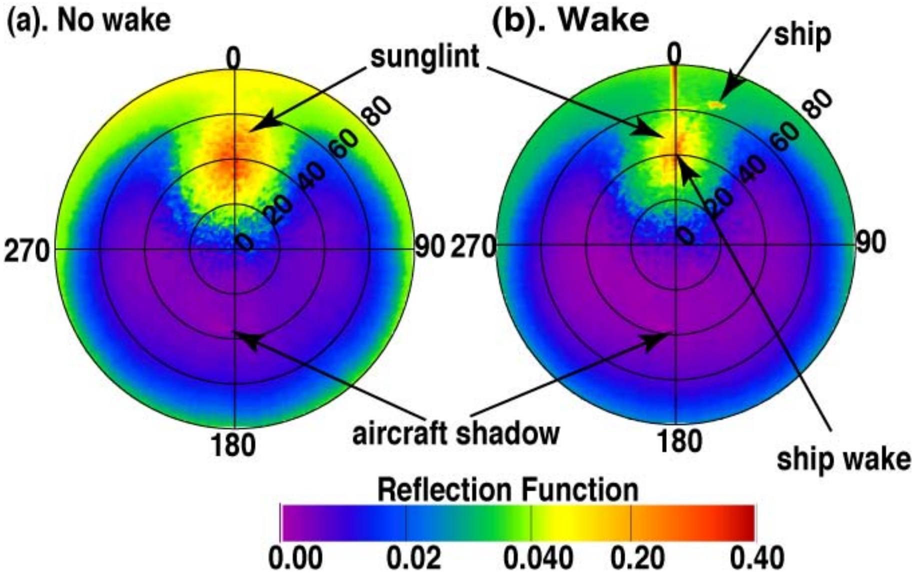

Fig. 2. Ocean bidirectional reflectance distribution function at 0.870 µm without and with ship wake. The ship wake measurements were made over a 294 m long cargo ship, which was moving through an area where the NASA P-3B aircraft was orbiting in a circular flight track at a constant altitude (~304 m above ocean surface).

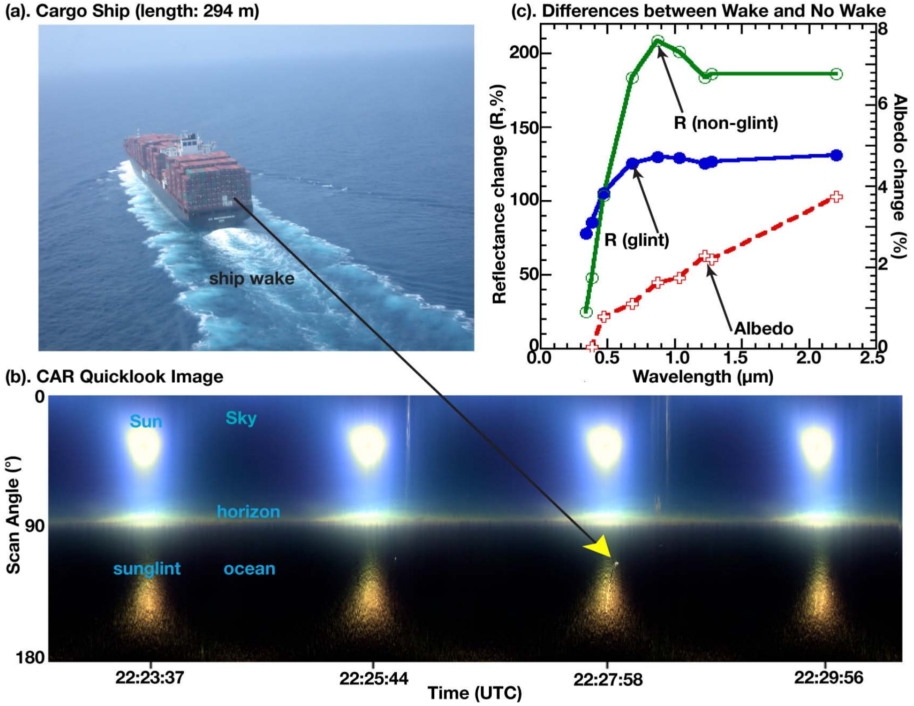

Fig. 3. **(a)** Cargo ship moving through the scene during airborne measurements. **(b)** The cargo ship can be seen in a quick-look image from NASA's Cloud Absorption Radiometer. **(c)** Change in reflectance in the solar principal plane (R_{glint}) and off-principal plane ($R_{\text{non-glint}}$) due to the presence of ship wake. The ship wake causes an increase in ocean reflectance in all directions as depicted by a change in glint and non-glint reflectance. The relative percentage increase of spectral albedo is from 1–4% in the visible and near-infrared wavelengths over an area >13 Km^2.